

TUNE EVALUATION IN SIMULATIONS AND EXPERIMENTS*

R. BARTOLINI¹, A. BAZZANI², M. GIOVANNOZZI¹, W. SCANDALE¹ and E. TODESCO³

¹*CERN, 1211 Geneva 23, Switzerland*

²*Dipartimento di Matematica, Piazza di Porta S. Donato 5, I-40126 Bologna*

³*INFN, Sezione di Bologna, Via Imerio 46, I-40126 Bologna*

(Received date to be inserted)

In circular accelerators, the betatron tune is measured by analysing the particle coordinates, sampled over N turns. Algorithms based either on the Average Phase Advance method or on the Fast Fourier Transform (FFT) are routinely used to compute the tune. More sophisticated approaches have recently been proposed. They rely on analytical interpolations of the FFT, as suggested by E. Asseo, or on algorithms based on continuous spectral analysis, according to the studies of J. Laskar. In this paper we critically review the various methods of measuring the tune and we present analytical estimates of the error as a function of N . The results are supported by numerical simulations carried out on both simple and complicated lattices, including nonlinear magnets. Applications to experimental data obtained in the CERN SPS are also shown.

1 INTRODUCTION

In circular accelerators, the choice of the working point strongly affects the stability of the particle motion. Therefore, in order to investigate the performances of a machine, one must have a precise knowledge of the value of the tune, i.e. of the ratio of the betatron over the revolution frequencies. There are various methods to evaluate the tune: an extensive review of them is given in Ref. ¹. In this paper, we consider the standard technique that requires to sample the transverse beam position for N turns and to perform an appropriate frequency analysis of the stored data. This method can be used both in theoretical studies and in routine operation. In the first case, one follows the particle trajectory for N turns, using numerical simulations. In the second case, one applies a fast deflection to the entire beam and observe the subsequent oscillations for N turns using a beam position monitor. In the following sections, we will describe extensively the algorithms by which one can compute the value of the tune from a set of N consecutive values of the transverse particle position. Our main concern will be to investigate in detail the frequency resolution that each algorithm can provide, when the values of the beam position are not affected by instrumental errors. This assumption will restrict the rigorous

* Work partially supported by EC Human Capital and Mobility contract Nr. ERBCHRXCT940480

validity of our formulae to the case of tracking studies. Applications to experimental measurements, affected by non-negligible instrumental errors, are still possible, at the expenses of some loss in frequency resolution, see Ref. ².

Two standard algorithms provide the tune from a time series of N consecutive values of the particle trajectory: the Average Phase Advance (APA), and the Fast Fourier Transform (FFT). The latter technique is quite standard and widely used in many applications. The former one is based on the reconstruction of the phase space of the particle trajectory and on the evaluation of the average angular progression per revolution. Both approaches have an intrinsic error proportional to $1/N$. In the practical cases, N is of the order of a thousand, and therefore the error of the tune is of the order 10^{-3} . This precision is fully satisfactory in routine operation.

However, in some applications one requires higher frequency resolution in as few turns as possible. For instance, this is essential to measure the detuning with the amplitude due to nonlinearities, whenever the initial beam deflection smears out too quickly, either by filamentation or by radiation damping. On the other hand, the time evolution of the instantaneous tune is useful to detect ripples or to reveal synchro–betatron coupling. In a recent work, J. Laskar ³ has pointed out some other relevant applications: the accurate tune evaluation over a wide sample of initial conditions can provide tune footprints containing clear informations on the global dynamics and on the width of resonances in a nonlinear machine ^{4,5,6}. Moreover, the change of the tune along the particle orbit has been suggested as an early indicator of chaoticity to speed up the investigations of the long-term stability ^{3,5}.

Remarkable attempts to improve the resolution of the tune computation using better algorithms were recently made by E. Asseo ⁷ and J. Laskar ⁴. The first method is based on the analytical interpolation of the FFT, whilst the second one relies on the search of the maximum of the continuous Fourier Transform. The interpolation technique was applied to measure the tune in the SPS ⁸ and in LEP ⁹ whilst the continuous Fourier Transform was recently used in SPEAR ¹⁰.

We will critically review the methods for precise tune estimate, giving a particular emphasis to those of Asseo and Laskar. We will present our estimates of the errors for the different techniques as a function of N . The analytical results are also supported by numerical simulations for both simple and complicated accelerator models containing nonlinear magnets. Moreover, experimental checks have been carried out on the CERN SPS, showing that the precision of the tune measurement can be considerably improved even for very small numbers of turns (i.e. $N = 16$).

The main results presented in this paper can be summarized as follows:

- An exact analytical interpolation of the FFT, which generalizes the approach of Asseo, has been worked out. The interesting feature of such an algorithm is that it is completely explicit.
- We showed that the error associated both with the interpolation and with the Laskar method is proportional to $1/N^2$; moreover, a substantial improvement can be obtained by using a filter. In the case of the Hanning filter we have worked out for both methods an estimate of the error proportional to $1/N^4$.

- We carried out numerical simulations for a wide variety of models that show that both the interpolation and the Laskar approach lead to similar results.
- We developed an interpolation procedure for the APA method which leads to a substantial improvement of the precision with respect to the plain APA.
- We showed that to separate two frequencies whose distance is $\Delta\nu$ one has to analyse at least N samples, with $N \geq 1/\Delta\nu$, independently of the algorithm.

The plan of the paper is the following. In Section 2 we describe the notations and in Section 3 we present the implemented models. In Section 4 we discuss the different methods for determining the tune and we outline an analytical estimate of the associated error. In Section 5 we apply these methods to determine the tunes in nonlinear mappings which model the betatron motion. We also analyse the tune estimate with a low number of samples, focusing on the models where the linear frequency is modulated. In Section 6 we apply the outlined methods to determine the precise value of the instantaneous tune to experimental data of a proton beam at the CERN SPS. Some proofs of the analytical estimates are left to the Appendices.

2 NOTATION

In this paper we will use the following notation: s is the coordinate along the accelerator azimuth; x, y are the coordinates in the plane perpendicular to s ; p_x and p_y are the momenta conjugated to x and y , i.e. their derivatives with respect to s . The particles progress in the four-dimensional phase space $x \equiv (x, p_x, y, p_y)$. Owing to the periodicity in s , it is customary to fix a particular section of the machine and to define the one-turn map M , which gives the positions and the momenta of the particle x' after one turn of the machine as a function of the initial values of the variables x :

$$x' = M(x) . \tag{1}$$

The phase space positions $x(n)$ at the n -th turn are then given by the successive application of the one-turn map n times; given an initial condition x , its orbit is the collection of its first N samples. We assume that the origin in phase space is a fixed point: $M(\mathbf{0}) = \mathbf{0}$ and that the linear part of M around $\mathbf{0}$ is stable, i.e. that it has four eigenvalues of modulus one ($e^{2\pi i\nu_x}, e^{-2\pi i\nu_x}, e^{2\pi i\nu_y}, e^{-2\pi i\nu_y}$). The frequencies ν_x and ν_y are the linear tunes of the betatron motion. For weak perturbations of the linear motion, the tunes are still well defined: indeed, one of the effects of nonlinearities is to introduce anharmonicity, i.e., to give a dependence of the tunes on the initial condition. We denote by $\nu_A(N)$ the estimate of the tune given by the method A using N samples of the orbit. The related error is given by $\epsilon_A(N) = \nu_A(N) - \nu_0$.

3 MODELS

In a first approximation, the motion of the particles in a circular accelerator can be considered linear, with each degree of freedom evolving in an independent manner along harmonic trajectories. Quite often, however, this model is insufficient. Well-known mechanisms, such as the linear, the non-linear, and the synchro-betatron coupling make more intricate the particle trajectory and mix together the three degrees of freedom. Additional orbit modulations eventually appear due to the unavoidable ripple of the main magnets. Nevertheless, in all the realistic cases, the frequency spectrum of an individual particle orbit is quite simple and only contains a numerable set of well isolated lines. They correspond to the eigenfrequencies of the motion and to their side-bands driven by coupling and ripple. Multiples of these fundamental peaks may also be present; however, their amplitude decrease very rapidly with the harmonic number, and therefore they can be neglected. We identified and described below five representative models of the particle orbits, that cover, in our opinion, most of the cases of interest. We will use them to produce simulated spectra for frequency analysis. The situation where the motion is strongly damped with time has not been considered, since it is extensively discussed in Ref. ¹⁵. Some care is required in analysing beams with many particles, especially when there is a finite frequency spread. Phenomena such as the Landau damping and the emittance filamentation destroy any coherent beam motion and can substantially modify the frequency response. However, the frequency analysis techniques are still applicable if the duration of the measurement is considerably shorter than the decoherence time.

The betatron motion is described in a separate manner for each degree of freedom. For instance the horizontal one is described in the two-dimensional phase space $x = (x, p_x)$, using the complex coordinate $z = x - ip_x$.

1) *One sine wave plus harmonics.* A simplified model of the orbit of a particle in a linear lattice is given by a sinusoidal wave of frequency ν_0 (which is the tune to be determined), plus a sum of its harmonics with complex weights a_k , of modulus smaller than one:

$$z(n) = e^{2\pi i \nu_0 n} + \sum_k a_k e^{2\pi i \nu_0 k n} \quad |a_k| < 1. \quad (2)$$

2) *Two sine waves plus harmonics.* To take into account the possible effect of horizontal-vertical coupling we use a more sophisticated model that contains a main sinusoidal wave of frequency ν_0 (with its harmonics), added to a secondary sinusoidal wave of frequency ν_1 (with its harmonics) with a complex weight of modulus smaller than one:

$$z(n) = e^{2\pi i \nu_0 n} + \sum_k a_k e^{2\pi i \nu_0 k n} + b_0 e^{2\pi i \nu_1 n} + \sum_k b_k e^{2\pi i \nu_1 k n} \quad |a_k|, |b_k| < 1. \quad (3)$$

Using this model, we will study the conditions to disentangle the frequency ν_0 from ν_1 .

- 3) *Modulated sine wave.* In order to simulate synchro-betatron coupling or tune modulation due to ripple of the power supplies, we use a sinusoidal wave whose frequency ν_0 is modulated at a frequency ν_m .

$$z(n) = \cos[2\pi\nu_0 n + A \sin(2\pi\nu_m n)]. \quad (4)$$

It is well known that a Fourier analysis of $z(n)$ gives the main peak at ν_0 plus a series of secondary peaks (called sidebands) displaced from ν_0 by an integer multiple of the modulation frequency ν_m . The above models will be used for both numerical simulations and analytical calculations. More realistic simulations will be performed for the following four-dimensional models.

- 4) *4D Hénon map.* It represents the transfer map of a FODO cell with a single sextupole in the thin lens approximation:

$$\begin{cases} x' &= \cos(2\pi\nu_x)x + \sin(2\pi\nu_x)[p_x + (x^2 - y^2)] \\ p_x' &= -\sin(2\pi\nu_x)x + \cos(2\pi\nu_x)[p_x + (x^2 - y^2)] \\ y' &= \cos(2\pi\nu_y)y + \sin(2\pi\nu_y)[p_y - 2xy] \\ p_y' &= -\sin(2\pi\nu_y)y + \cos(2\pi\nu_y)[p_y - 2xy] \end{cases} \quad (5)$$

where ν_x and ν_y are the linear tunes.

- 5) *SPS lattice.* The lattice used represents the set-up for nonlinear dynamics experiments¹¹. The nonlinear part of the magnetic lattice is made up of eight strong sextupoles normally used to extract the beam, and of 108 chromatic sextupoles placed near the main quadrupoles of the regular cells. The linear tune is set to $\nu_x = 26.605$ and $\nu_y = 26.538$, which is close to resonances of 5th order.

4 TUNE DETERMINATION AND ERROR ESTIMATE

4.1 Average Phase Advance (APA) methods

We will present here the definition of the Average Phase Advance and the estimates of the associated tune error. Improvements can be obtained through fitting procedures or by removing the phase space nonlinear distortion by the use of normal forms. Numerical evidence of the behaviour of the APA methods will be presented in Section 5.

4.1.1 Average phase advance The Average Phase Advance (see Ref.¹²) is a method used to compute the frequency of an orbit of a dynamical system in the neighbourhood of an elliptic fixed point. In fact, in the theory of quasi-integrable dynamical systems the APA is taken as the definition of nonlinear frequency (which is usually called rotation number¹³). According to the APA method, given a 2D

orbit $x(n)$ with $n = 1, \dots, N$, the tune is given by the average of θ_n :

$$\nu_{APA}(N) = \frac{1}{2\pi(N-1)} \sum_{n=2}^N \theta_n, \quad (6)$$

where θ_n is the phase advance between the iterate $n-1$ and the iterate n . The resolution in tune of the APA method will be studied using the signal of Eq. (3), made of the sum of two sinusoidal waves without harmonics. Our deductions are summarized below, and additional considerations are presented in Appendix A

- For generic ν_0 , ν_1 and b_0 , the error is proportional to the inverse of the number of samples:

$$|\epsilon_{APA}(N)| \leq \frac{C_{APA}}{N-1} \quad C_{APA} \leq \frac{1}{2}. \quad (7)$$

- If $|b_0| \ll 1$ (small perturbations of the linear case), the constant C_{APA} is proportional to the perturbation strength:

$$|b_0| \ll 1 \quad \Rightarrow \quad C_{APA} \leq \frac{|b_0|}{2\pi}; \quad (8)$$

therefore, in the linear case the APA provides the tune with infinite precision.

- If the distance between the frequencies $\Delta\nu = \nu_0 - \nu_1$ is small compared with the inverse of the number of samples, one cannot separate the two frequencies, and the error is independent of N :

$$|N\Delta\nu| < 1 \quad \Rightarrow \quad |\epsilon_{APA}(N)| \leq \Delta\nu \frac{|b_0|}{|1+b_0|}. \quad (9)$$

4.1.2 Fitted averaged APA In order to improve the convergence properties of the APA method, one has to analyse the features of $\nu_{APA}(N)$ versus N ; in Fig. 1(a) we plot this function for a simplified orbit that follows Eq. (2); the convergence to the asymptotic value is reached with damped oscillations around the limiting value. One can get rid of the periodic component in $\nu_{APA}(N)$ by considering the averaged tune, i.e.

$$\langle \nu_{APA}(n) \rangle = \frac{1}{n-1} \sum_{m=2}^n \nu_{APA}(m) \quad n = 2, \dots, N. \quad (10)$$

The plot of $\langle \nu_{APA}(n) \rangle$, presented in Fig. 1(b), shows that the error of the averaged APA is very close to an hyperbola: therefore one can give a better estimate by fitting the averaged APA with a linear regression

$$\langle \nu_{APA}(n) \rangle \approx \nu_{Afit}(N) + \frac{A}{n-1} \quad n = 2, \dots, N; \quad (11)$$

here $\nu_{Afit}(N)$ is the tune estimated by the fitting using N samples of the orbit, and A is a constant. It will be shown by simulations that this method allows one to improve the scaling law of the error

$$|\epsilon_{Afit}(N)| \leq \frac{C_{Afit}}{N^2}. \quad (12)$$

4.1.3 APA over normal forms Another way to improve the APA method is based on the perturbative tools¹⁴. According to the normal form theory¹², it is possible to determine a coordinate transformation such that in the new variables the dynamics shows explicitly its symmetries. If the APA method is applied over the orbit transformed using normal forms, one obtains a better estimate since the distortion of the orbits due to nonlinear effects is smaller, and therefore the constant in the error is reduced:

$$|\epsilon_{Anf}(N)| \leq \frac{C_{Anf}}{N} \quad C_{Anf} < C_{APA}. \quad (13)$$

The effectiveness of this approach diminishes as the distance of the orbit from the origin is increased: in fact, at large amplitudes the nonlinearities are stronger. Moreover, one has to take into account that the perturbative series are divergent, and therefore the unavoidable truncation introduces small approximations which will affect the precision of the tune evaluation.

4.2 Fourier Series methods

4.2.1 Fourier Series (FS) Another method routinely used in the analysis of signals, is based on the Fourier Series (FS). A signal $\{z(1), z(2), \dots, z(N)\}$, where $z(n)$ is one of the coordinates of the orbit, can be expanded as a linear combination of a finite number of orthonormal functions:

$$z(n) = \sum_{j=1}^N \phi(\nu_j) \exp(2\pi i n \nu_j) \quad \nu_j = \frac{j}{N}; \quad (14)$$

the coefficients $\phi(\nu_j)$ are given by the inverse formula

$$\phi(\nu_j) = \frac{1}{N} \sum_{n=1}^N z(n) \exp(-2\pi i n \nu_j). \quad (15)$$

The sequence of the N coefficients $\phi(\nu_j)$ is the FS of the orbit; their absolute values $|\phi(\nu_1)|, \dots, |\phi(\nu_N)|$ are the amplitude spectrum of $z(n)$. The frequency can be evaluated as the abscissa of the main peak in the amplitude spectrum, i.e., the value of ν_j which maximizes $|\phi(\nu_j)|$. Let us recall some well-known properties of the FS:

- using the procedure, we implicitly assume that the N samples $z(n)$ are in fact extended in a periodic sampled signal of period N ;
- the spectrum is therefore discrete and periodic of period N , since it contains a *finite* set of independent modes $e^{2\pi i \nu_j}$ with $\nu_j = 1/N, 2/N, \dots, (N-1)/N, 1$;
- if the signals have real values, the spectrum is mirror-symmetric around one half in the frequency range $[0, 1]$.

4.2.2 Fast Fourier Transform (FFT) In principle, the computation of the FS for a signal of N samples requires N^2 operations; indeed, if N is a power of two, one can define an algorithm that computes the FS by using only $N \log N$ operations:

this method is called the Fast Fourier Transform (FFT), and is widely used in many different fields of physics and engineering.

The error associated with the FFT is due to the discreteness of the values of ν_j , and therefore is given by

$$|\epsilon_{FFT}| \leq \frac{C_{FFT}}{N} \quad \text{where} \quad N = 2^M \quad C_{FFT} = \frac{1}{2}. \quad (16)$$

The main advantage of the FFT is to provide a very fast estimate of the complete Fourier spectrum, even though the direct evaluation of the main frequency is poor. Moreover, contrary to the APA, the error is independent of the nonlinearity of the system, and it does not tend to zero when the nonlinearities become small. In the next subsection we will show how to improve the precision by using very simple analytical tools.

4.2.3 Interpolated FFT Since the error in the FFT estimate is due to the discreteness of the spectrum, one can try to obtain better results by interpolating it around the main peak. The tune is then the abscissa of the maximum of the interpolating function. Following the approach outlined by Asseo^{7,15,16}, we use as interpolating function the spectrum of a pure sinusoidal signal with unknown frequency ν_{Fint} :

$$|\phi(\nu_j)| = \left| \frac{\sin N\pi(\nu_{Fint} - \nu_j)}{N \sin \pi(\nu_{Fint} - \nu_j)} \right|. \quad (17)$$

The explicit expression of the tune is:

$$\nu_{Fint} = \frac{k}{N} + \frac{1}{\pi} \arctan \left(\frac{|\phi(\nu_{k+1})| \sin(\pi/N)}{|\phi(\nu_k)| + |\phi(\nu_{k+1})| \cos(\pi/N)} \right). \quad (18)$$

In the case of a sum of sinusoidal waves [see Eq. (3)], the error associated with this method for large N and distance between the main frequency and the closest one larger than N^{-1} is

$$|\epsilon_{Fint}| \leq \frac{C_{Fint}}{N^2}. \quad (19)$$

From Asseo *et al.*⁷ the formula for the interpolated tune reads

$$\nu_{Fint} = \frac{k}{N} + \frac{1}{N} \frac{|\phi(\nu_{k+1})|}{|\phi(\nu_k)| + |\phi(\nu_{k+1})|}. \quad (20)$$

This expression has been derived directly from

$$|\phi(\nu_j)| \approx \frac{1}{N} \left| \int_0^N e^{2\pi i k(\nu_0 - \nu_j)} dk \right| = \left| \frac{\sin N\pi(\nu_0 - \nu_j)}{N\pi(\nu_0 - \nu_j)} \right| \quad (21)$$

in the specific case $j = k, k + 1$.

In fact it is easy to show that Eq. (20) can be derived by expanding Eq. (B.2) in power series of N^{-1} and neglecting $O(N^{-3})$.

The arguments used to prove rigorously Eqs. (18) and (19) will be given in Appendix B.1. Our result modifies the interpretation quoted¹⁵, where only a

dependence on $1/N$ of ϵ_{Fint} was found. Furthermore, our estimate agrees with those reported by Schmickler⁹, where the dependence on $1/N^2$ was found, but it was explained phenomenologically as the effect of the electronic noise. More general cases are treated numerically in Sect. 5. Other types of interpolating functions have been proposed in the literature, such as a parabola¹⁷; in this case one needs three spectra values to make the interpolation. Even though the parabola is not optimal, it provides some gain with respect to the plain FFT. A discussion of this method and of the associated error is given in Appendix B.2.

4.2.4 Interpolated FFT with data windowing A standard approach used in signal processing theory to improve the Fourier analysis is based on filtering the data $z(n)$ using weight functions $\chi(n)$ (see Laskar³ and Harris¹⁸). In this case, the FS of the orbit reads

$$\phi(\nu_j) = \frac{1}{N} \sum_{n=1}^n z(n) \chi(n) \exp(-2\pi i n \nu_j). \quad (22)$$

We consider a Hanning filter

$$\chi(n) = 2 \sin^2 \left(\frac{\pi n}{N} \right); \quad (23)$$

then, the spectrum of a pure sinusoidal signal of frequency ν_0 is

$$|\phi(\nu_j)| = \left| \frac{\sin^2(\pi/N) \sin \pi N(\nu_0 - \nu_j) \cos \pi(\nu_0 - \nu_j)}{N \sin \pi(\nu_0 - \nu_j) \sin \pi(\nu_0 - \nu_j + \frac{1}{N}) \sin \pi(\nu_0 - \nu_j - \frac{1}{N})} \right|. \quad (24)$$

With respect to the case without filter, one has two effects: the width of the main peak centred at ν_0 is increased from $2/N$ to $4/N$; moreover, for large N the height of the peaks that are far from the main one is reduced from $1/N$ to $1/N^3$. This second feature allows one to reduce considerably the influence of next-to-leading frequencies, which are the main sources of error in the determination of the tune. One can define higher order windows $\chi_l(n) \propto \sin^l(\pi n/N)$, with $l > 2$; for high l the broadening of the main peak width becomes dominant over the reduction of the influence of the secondary harmonics, and therefore no improvement in the precision of the tune estimate is obtained. The Hanning filter proves to be one of the optimal filters (see also Harris¹⁸).

By applying the same reasoning used for the case of the interpolated FFT, it is possible to show that the expression of the tune is:

$$\nu_{FHan} = \frac{k}{N} + \frac{1}{2\pi} \arcsin \left[A \left(|\phi(\nu_k)|, |\phi(\nu_{k+1})|, \cos \frac{2\pi}{N} \right) \sin \frac{2\pi}{N} \right], \quad (25)$$

where the function A is given by

$$A(a, b, c) = \frac{-(a + bc)(a - b) + b\sqrt{c^2(a + b)^2 - 2ab(2c^2 - c - 1)}}{a^2 + b^2 + 2abc}. \quad (26)$$

Moreover the error scales as:

$$|\epsilon_{Fint}| \leq \frac{C_{FHan}}{N^4}. \quad (27)$$

The proof is given in Appendix B.3.

4.3 Fourier Transform methods

4.3.1 Fourier Transform (FT) Another very effective approach which has been extensively used in the literature ^{3,4,5,10} is based on the Fourier Transform (FT). Let us consider a continuous function $f(t)$, where $t \in R$. Then, it can be expanded as a linear combination of an infinite number of orthonormal functions:

$$f(t) = \int_{-\infty}^{+\infty} \phi(\nu) \exp(2\pi i\nu t) d\nu. \quad (28)$$

The function $\phi(\nu)$ is the FT of $f(t)$, and is given by the inverse formula

$$\phi(\nu) = \frac{1}{N} \int_0^N f(t) \exp(-2\pi i\nu t) dt. \quad (29)$$

The main frequency of the function $f(t)$ is given by the abscissa of the maximum of the function ϕ . The FT provides a much better estimate than the plain FFT, since in this case the frequency ν varies over an interval and not over a finite set of points.

In our case we have a discrete system whose orbit $z(n)$ is defined only for integer times. Therefore one has to replace the integral with a finite sum in Eqs. (28) and (29):

$$\phi(\nu) = \frac{1}{N} \sum_{n=0}^N z(n) \exp(-2\pi i\nu n). \quad (30)$$

This definition is equal to the FS [see Eq. (15)]; the only difference is that now ν is a continuous variable. The position of the maximum of $|\phi|$ provides the tune estimate. Contrary to the case of the interpolated FFT, no analytical formulas are available; indeed, the maximum can be computed, using ν_{FFT} as a first guess, through a standard numerical approach such as the bisection method or the Newton method.

The FT provides a tune estimate that has infinite precision for the linear case. In Appendix C we give an analytical estimate of the error for the case of a sum of sine waves. For the sake of simplicity, the case of a continuous orbit $f(t)$ has been analysed: the same results hold for the discrete case. One finds the same scaling laws as in the case of the interpolated FFT.

- For large N , provided that the distance $\Delta\nu$ between the main frequency and the closest one is greater than $1/N$, one has

$$|\epsilon_{FT}| \leq \frac{C_{FT}}{N^2}. \quad (31)$$

- If $\Delta\nu N < 1$, the error is independent of N and one obtains the same estimate that holds for the APA [see Eq. (9)].

4.3.2 FT and data windowing As usual, data windowing considerably improves the precision of the method: one defines a FT as

$$\phi(\nu) = \frac{1}{N} \sum_{n=0}^N z(n)\chi(n) \exp(-2\pi i\nu n) \quad (32)$$

where $\chi(n)$ is a window function. In the case of a Hanning window [see Eq. (23)] one obtains an error estimate which scales like N^{-4} :

$$|\epsilon_{FTHan}| \leq \frac{C_{FTHan}}{N^4}. \quad (33)$$

This result is proved for a continuous signal in Appendix C.2 and has been checked numerically (see Figs. 2–6). A similar proof can be given for the discrete case. Our estimate differs from that of Laskar³, where only the depression of the perturbing secondary maxima, proportional to $1/N^3$, was taken into account.

5 NUMERICAL RESULTS

The effectiveness of the methods and the error estimates for tune evaluations have been checked numerically on the models presented in Sect. 3. All the figures are in double logarithmic scale.

5.1 Sine waves

We use the signal of Eq. (2) with main frequency $\nu_0 = 0.28$, and four harmonics with exponentially decreasing amplitudes $a_k = e^{-k}$.

In Fig. 2 we plot the behaviour of the error $\epsilon_A(N)$ versus the iteration time N for the different methods. In Fig. 2(a) the improvement of the precision due to the fit performed on the APA method is apparent. The very small error (about 10^{-15}) for some special values of N is the effect of some cancellations due to the too simple structure of the analysed signal. In Fig. 2(b) the three regimes of the different types of Fourier analysis (i.e. $\epsilon(N) \propto 1/N$, $1/N^2$, $1/N^4$) are clearly visible. The stepwise decrease of $\epsilon_{FFT}(N)$ corresponds to $N = 2^M$ for integer M . The results of the FS with interpolation and of the FT are very similar. Note that with this model the exact value of the tune is a priori known, being an input parameter of the signal.

Let us now consider model 2); the main tunes are set to the values $\nu_0 = 0.28$ and $\nu_1 = 0.31$ corresponding to the linear frequency of the planned LHC. The main amplitude of the second frequency is arbitrarily set to 0.25. For each tune, four harmonics of exponentially decreasing amplitude are included. The results of the simulations are shown in Fig. 3. As in the previous case the error scales according to the expected power laws.

By choosing ν_1 closer to ν_0 , one can see that $\epsilon(N)$ becomes constant as the condition $N\Delta\nu > 1$ is not fulfilled. This effect is clearly shown in Fig. 4 corresponding to $\nu_0 = 0.28$ and $\nu_1 = 0.281$. The plateau of $\epsilon(N)$ is visible up to $N = 10^3$. Similar results have been obtained for $\Delta\nu = 10^{-4}$, where the plateau is lengthened up to $N = 10^4$.

5.2 4D Hénon map

We consider the evaluation of the tune in the 4D Hénon map [see Eq. (5)]. Orbits with initial conditions either near the origin or close to the border of the dynamic aperture are investigated. In both cases the initial values of the horizontal and vertical positions are identical, whilst the conjugated momenta are set to zero. Since the tune at a finite value of the amplitude is not known a priori, we conventionally decide to evaluate it by means of the FT method with Hanning filter for $N = 10^5$ samples. The tune error is then the difference from these conventional values.

In Fig. 5 the various estimates of the tune as a function of N for initial conditions at $1/10$ [Fig. 5(a)] and $9/10$ (Fig. 5(b)) of the dynamic aperture are shown. The scaling laws are fully confirmed as for the previous cases. Furthermore, using the APA method combined with normal forms we find an extremely precise determination of the tune even for a very small number of turns, although the scaling law is still proportional to $1/N$. This implies that the proportionality constant C_{Anf} is very small. In addition the data of Fig. 5 show that C_{Anf} strongly depends on the initial amplitude of the orbit: the improvement becomes considerably smaller close to the dynamic aperture.

5.3 SPS lattice

Simulations have been performed on a realistic model of the CERN SPS with strong perturbing sextupoles, residual linear coupling, and without accelerating RF or tune modulation. The initial values of the horizontal and vertical positions are chosen at half of the dynamic aperture, and the conjugated momenta have been set to zero. As in the previous subsection, the reference value of the tune is that obtained with the FT method and the Hanning filter in 10^5 turns. In Fig. 6 the errors for the different methods are presented. They confirm the scaling laws already discussed. The asymptotic value of the error tends to zero for N large. However, one usually find a finite threshold due to computer precision. For sine wave and the Hénon map this threshold corresponds to the machine accuracy (10^{-16}) as shown in Figs. 2–5. For the SPS lattice, however, this value is of the order of 10^{-10} , probably because of the much larger number of operations required to perform the tracking.

5.4 Frequency-modulated sine wave

In this section we numerically analyse a sine wave whose tune ν_0 is modulated by a secondary frequency ν_m [see Eq. (4)]; we fixed $\nu_0 = 0.6$, $\nu_m = 0.005$ and $A = 0.1$. For N large enough to resolve the sidebands from the fundamental oscillation, i.e.,

for $N \geq 1/\nu_m$, the tune error follows the usual scaling laws. But, when $N < 1/\nu_m$, the value of the tune is no longer well defined. To clarify this, let us consider a signal that contains pN samples. We can subdivide them into p samples, each containing N samples and compute with them p consecutive values of the tune. These values oscillate around ν_0 with frequencies that are harmonics of ν_m . An example of this is shown in Figs. 7 and 8. In Fig. 7 the plain FFT over $N = 2048$ is shown; in Fig. 8(a) we plot the tune computed over $p = 128$ samples of $N = 16$ samples. We consider this plot as a new time series and apply to it an FFT: the resulting spectrum presented in Fig. 8(b) shows the low harmonics of ν_m . This behaviour is independent of the choice of the modulating frequency and of the value of N , provided that $N < 1/\nu_m$. Analogous results have been obtained for a 4D Hénon map with modulated linear frequency. The procedure outlined here, with the academic interest of clarifying the definition of the instantaneous tune, will be applied to the experimental data in Sect. 6.

6 EXPERIMENTAL RESULTS

The algorithms for tune measurements have also been tested on experimental data. We use proton beams during the rise of the magnetic field at an energy of about 400 GeV during normal operation. The horizontal and vertical tunes are close to 0.62 and 0.58, respectively, the chromaticities are close to zero ($Q'_{x,y} \approx 2$), and the closed orbit is well compensated (r.m.s. deviation approximately 0.5 mm). After a single-turn kick deflection, the value of the transverse position is stored for 1024 turns. An example of data relative to the vertical motion is given in Fig. 9(a). The amplitude of the beam oscillation is decreasing, due to the presence of an active transverse feedback used to avoid coherent particle motion. The FFT spectrum of the vertical betatron oscillations is shown in Fig. 9(b). The main peak corresponds to the tune $\nu_y = 0.5830$. Sidebands are clearly seen, corresponding to a tune modulation $\nu_m = 0.011$. The error associated with the FFT over 1024 turns is 0.0005. By interpolating the FFT with Hanning filter to the whole series of 1024 data we get $\nu_y = 0.58319$ in agreement with the FFT (see Tab. 1) within the error. We then considered the first 128 turns: the precision of the FFT drops to 0.004, whilst the interpolating and filtered FFT gives a tune which is still in agreement with the values calculated with 1024 turns.

For $N < 128$, the main peak can no longer be disentangled from the sidebands and the measure of the tune is affected by the presence of the modulation. Indeed, subdividing the 1024 data in $p = 64$ samples of $N = 16$ values and computing for each of them the tune, one can see an oscillation around the mean value 0.58322 of amplitude within ± 0.003 [see Fig. 10(a)]. The spectrum of this signal is shown in Fig. 10(b): one observes the harmonics of the modulating frequency ν_m . This is in agreement with the behaviour illustrated for the frequency-modulated signal given in Sect. 5.4. Notwithstanding the presence of the ripple, there is a considerable improvement also for an extremely low number of turns: one can observe from Fig. 10(a) that, using this method, the error of the tune estimate over 16 turns

TABLE 1: Tune estimates for the SPS.

N	FFT	Interp. FFT + Hanning
1024	0.5830 ± 0.0005	0.58319
128	0.585 ± 0.004	0.5832
16	0.56 ± 0.03	0.585

is always bounded by ± 0.003 , i.e., one order of magnitude less than the error associated with the corresponding FFT (see Tab. 1).

These examples show that also in experiments a precise measure of tune can be performed with interpolation and filtering techniques, substantially reducing the requested number of turns. The same considerations are valid for the approach based on the FT plus Hanning filter.

7 CONCLUSIONS

We presented here a complete overview of the methods used to determine the betatron tune in circular particle accelerators. They are essentially based on well-assessed concepts of Fourier analysis, the most popular of which is the FFT, a simple and powerful algorithm, widely used to compute the spectrum of the betatron oscillations. We pointed out that recent applications, mostly related to the analysis of nonlinear effects, require more precision than allowed by plain FFT. We described the methods to increase the tune precision (interpolated FFT proposed by Asseo, NAFF³ proposed by Laskar) and we worked out in detail the scaling laws of the error as a function of the available number N of iterations. Our effort was oriented to show analytical and numerical evidence of these scaling laws, rather than specific applications.

Our experimental analysis was on purpose concise and rather academic in order to corroborate the theoretical results with real measurements in standard operating conditions. However, we cannot refrain from stressing that the applications of the modern methods of Fourier analysis discussed here are extremely appealing both in experimental and numerical studies of beam dynamics. These methods are certainly propaedeutic to a deeper investigation of existing or planned accelerators, for instance:

- to study the global beam stability in the CERN LHC by dense-tune footprints⁶,
- or to measure the detuning with the amplitude in CERN LEP, at the highest energy, in presence of fast radiation damping.

These investigations require robust algorithms that are able to provide in a simple manner the precise tune value of the instantaneous betatron tune.

ACKNOWLEDGEMENTS

We would like to thank J. Laskar, whose work has inspired our analysis, for useful and constructive discussions. We would also like to thank J. Gareyte for the support and J.P. Koutchouck, H.J. Schmickler, and A. Verdier for drawing our attention to the work by E. Asseo (which in our opinion has not been sufficiently disseminated). A special thank-you to M. Bassetti, C. Cornacchia, S. Kamada, L. Pellegrini, F. Ruggiero, M. Serio, P. Tran, and G. Turchetti for useful remarks and comments on the paper. We would like to express our warm gratitude to L. Jensen and G. Buur for the measurements performed at the CERN SPS. Finally, the authors are grateful to the DTP for the efficient work in preparing this report.

REFERENCES

1. M. Serio, CERN **91-04** 136–160.
2. R. Bartolini et al., ‘Precise Measurement of the Betatron Tune’, presented at LHC95, Montreux, October 1995.
3. J. Laskar, C. Froeschlé and A. Celletti, *Physica D* **56** (1992) 253
4. J. Laskar, *Physica D* **67** (1993) 257
5. H. S. Dumas and J. Laskar, *Phys. Rev. Lett.* **70** (1993) 2975
6. M. Giovannozzi, R. Grassi, W. Scandale and E. Todesco, *Phys. Rev. E* **52** (1995), in press
7. E. Asseo, J. Bengtsson and M. Chanel, in *Fourth European Signal Processing Conference*, edited by J. L. Lacoume et al. (North Holland, Amsterdam, 1988) pp. 1317–20
8. H. Jakob et al., CERN SL **95-68(BI)** (1995)
9. H. J. Schmickler, CERN LEP Note (BI) **87-10** (1987)
10. P. Tran et al., submitted to the PAC Conference, Dallas, 1995
11. J. Gareyte, W. Scandale and F. Schmidt, in *Nonlinear Problems in Accelerator Physics*, edited by M. Berz et al. (Institute of Physics, Bristol, 1992) Conference Series 131, pp. 235–48
12. A. Bazzani, E. Todesco, G. Turchetti and G. Servizi, CERN **94-02** (1994)
13. R. S. MacKay, in *Nonlinear Dynamical Aspects of Particle Accelerators*, edited by J. M. Jowett, M. Month and S. Turner (Springer Verlag, New York, 1985) pp. 390–454
14. J. Miles, CERN SL (AP) Note **95-36** (1995)
15. E. Asseo, CERN PS Note (LEA) **85-9** (1985)
16. E. Asseo, CERN PS Note (LEA) **87-1** (1987)
17. S. Kamada, KEK Preprint **94-176** (1994)
18. F. J. Harris, *Proc. IEEE* **66** (1978) 51

APPENDIX A

Appendix A ERROR ESTIMATES FOR THE APA METHOD

In this section we prove the error estimates of the APA method for a simplified orbit that is made up of a linear combination of two sinusoidal waves:

$$z(n) = e^{2\pi i\nu_0 n} + b_0 e^{2\pi i\nu_1 n}, \quad |b_0| < 1 \quad n \in N; \quad (\text{A.1})$$

we express $z(n)$ as

$$z(n) = A_n e^{i\phi_n}, \quad (\text{A.2})$$

where

$$\begin{aligned} A_n &= \sqrt{1 + 2b_0 \cos 2\pi n \Delta\nu + b_0^2} \\ \phi_n &= \nu_0 n - \frac{1}{2\pi} \arctan \frac{b_0 \sin 2\pi n \Delta\nu}{1 + b_0 \cos 2\pi n \Delta\nu} \end{aligned}$$

and $\Delta\nu = \nu_0 - \nu_1$. We have assumed that b_0 is real: this assumption is not restrictive and one can prove that in the general case, b_0 complex, one obtains the same results. The tune estimate given by the APA method is

$$\nu_{APA}(N) = \frac{1}{N-1} \sum_{j=2}^N (\phi_j - \phi_{j-1}) = \frac{1}{N-1} (\phi_N - \phi_1); \quad (\text{A.3})$$

then, shifting the origin of the angles in order to set $\phi_1 = \nu_0$, one obtains

$$\nu_{APA}(N) = \nu_0 - \frac{1}{2\pi(N-1)} \arctan \frac{b_0 \sin 2\pi N \Delta\nu}{1 + b_0 \cos 2\pi N \Delta\nu}. \quad (\text{A.4})$$

One can give the following estimates.

- In all cases, since the arc tangent is bounded by π , one has the estimate

$$|\epsilon_{APA}(N)| \leq \frac{1}{2(N-1)}. \quad (\text{A.5})$$

- If the second frequency has a very small amplitude $|b_0| \ll 1$, one can expand Eq. (A.4) at the first order:

$$\nu_{APA}(N) = \nu_0 - \frac{b_0}{2\pi(N-1)} \sin 2\pi N \Delta\nu + O(|b_0|^3) \quad (\text{A.6})$$

and therefore one obtains

$$|\epsilon_{APA}(N)| \leq \frac{|b_0|}{2\pi(N-1)} \quad |b_0| \ll 1. \quad (\text{A.7})$$

This corresponds to the limit for weak nonlinearity.

- If $\Delta\nu$ is very small compared to the inverse of the number of the samples N^{-1} , then one can expand the trigonometric functions at first order in $N\Delta\nu$:

$$\nu_{APA}(N) = \nu_0 - \Delta\nu \frac{b_0}{1+b_0} \frac{N}{N-1} + O(|N\Delta\nu|^2) \quad (\text{A.8})$$

therefore the error is approximately independent of the number of samples (as long as the condition $|N\Delta\nu| \ll 1$ is satisfied):

$$|\epsilon_{APA}(N)| \leq |\Delta\nu| \frac{2|b_0|}{|1+b_0|} . \quad (\text{A.9})$$

APPENDIX B

B ERROR ESTIMATES FOR THE FS METHOD

B.1 FFT with sine interpolation

The starting point of our analysis is the interpolating function (17). Let $\phi(\nu_k)$ and $\phi(\nu_{k+1})$ be the main peak and its largest neighbourhood of a generic spectrum. Then, the interpolation procedure gives

$$\frac{|\phi(\nu_k)|}{|\phi(\nu_{k+1})|} = -\frac{N \sin \pi(\nu_{Fint} - (k+1)/N)}{N \sin \pi(\nu_{Fint} - k/N)} \quad (\text{B.1})$$

whose solution reads

$$\nu_{Fint} = \frac{k}{N} + \frac{1}{\pi} \arctan \left(\frac{|\phi(\nu_{k+1})| \sin(\pi/N)}{|\phi(\nu_k)| + |\phi(\nu_{k+1})| \cos(\pi/N)} \right). \quad (\text{B.2})$$

This formula provides the exact frequency in the case of a linear system.

In the case of a generic signal, made up by the sum of many sine waves, we have to take into account the effect of the secondary frequencies on the coefficients $\phi(\nu_k)$ and $\phi(\nu_{k+1})$. Using the interpolating function shown in Eq. (17) one can see that the new coefficients $\phi(\nu_k)$ differ by the old ones by a term proportional to $1/N$. Therefore Eq. (B.2) will read

$$\bar{\nu}_{Fint} = \frac{k}{N} + \frac{1}{\pi} \arctan \left(\frac{\sin(\pi/N) |\phi(\nu_{k+1}) + O(N^{-1})|}{|\phi(\nu_k) + O(N^{-1})| + |\phi(\nu_{k+1}) + O(N^{-1})|} \right). \quad (\text{B.3})$$

The final estimate (19) can be obtained by expanding again the previous equation and using Eq. (B.2)

$$\bar{\nu}_{Fint} = \nu_{Fint} + O(N^{-2}). \quad (\text{B.4})$$

B.2 FFT with parabolic interpolation

In this section we explicitly work out the tune estimate through the FFT with parabolic interpolation and the associated errors. Let us start with the interpolating function of a linear signal given by Eq. (17). The width of its main peak is $2/N$ therefore it contains only two bins of the plain FFT. We select the main peak $|\phi(\nu_k)|$ and its neighbour $|\phi(\nu_{k-1})|$ and $|\phi(\nu_{k+1})|$, assuming that $|\phi(\nu_{k+1})|$ is the smallest we change its sign. We interpolate these three peaks with a parabola $y = ax^2 + bx + c$; substituting the interpolating points $(\nu_{k-1}, |\phi(\nu_{k-1})|)$, $(\nu_k, |\phi(\nu_k)|)$ and $(\nu_{k+1}, -|\phi(\nu_{k+1})|)$, one obtains a system that determines the constants a, b, c . The interpolated tune reads

$$\nu_{Fpar} = -\frac{b}{2a} = \frac{k}{N} + \frac{1}{2} \frac{|\phi(\nu_{k+1})| + |\phi(\nu_{k-1})|}{|\phi(\nu_{k+1})| - 2|\phi(\nu_k)| + |\phi(\nu_{k-1})|}. \quad (\text{B.5})$$

A comparison with the exact solution (B.2) shows that the above formula is affected by an error which is $O(N^{-1})$. If we use the Hanning filter, the central peak of the interpolating function in Eq. 24 contains three bins of the plain FFT, therefore the interpolating points are $(\nu_{k\pm 1}, |\phi(\nu_{k\pm 1})|)$ and $(\nu_k, |\phi(\nu_k)|)$. The final result will, however, be affected by an error $O(N^{-1})$.

B.3 FFT with sine interpolation and data windowing

Following the same approach used in Appendix B.1, we compute the FFT of a filtered orbit, and we select the main peak and its largest neighbour $\phi(\nu_k)$ and $\phi(\nu_{k+1})$; then, we make an interpolation using the explicit solution worked out for the linear case [see Eq. (24)], where ν_0 is replaced by the tune estimate ν_{FHan} . One obtains the following equation

$$\frac{|\phi(\nu_k)|}{|\phi(\nu_{k+1})|} = -\frac{\cos \pi(\nu_{FHan} - k/N) \sin \pi(\nu_{FHan} - (k+2)/N)}{\cos \pi(\nu_{FHan} - (k+1)/N) \sin \pi(\nu_{FHan} - (k-1)/N)} \quad (\text{B.6})$$

whose solution is given in Eq. (25).

In the case of a sum of sine waves, applying arguments similar to those used in Appendix B.1, it can be shown that the secondary frequencies affect the Fourier coefficients by an error which is $O(N^{-3})$: this is a direct consequence of the presence of the filter. Therefore Eq. (25) can be recast in the following form

$$\bar{\nu}_{FHan} = \frac{k}{N} + \frac{1}{2\pi} \arcsin \left[A \left(|\phi(\nu_k) + O(N^{-3})|, |\phi(\nu_{k+1}) + O(N^{-3})|, \cos \frac{2\pi}{N} \right) \sin \frac{2\pi}{N} \right]. \quad (\text{B.7})$$

By expanding the previous equation one obtains the final result

$$\bar{\nu}_{FHan} = \nu_{FHan} + O(N^{-4}), \quad (\text{B.8})$$

which proves the estimate (27).

APPENDIX C

C ERROR ESTIMATES FOR THE FT METHODS

C.1 Fourier Transform

In this Appendix we evaluate the error estimate of the tune computed through the FT method [see Sect. (4.3.1)] in the case of a continuous signal $z(t)$, where $t \in [-N/2, N/2]$. Let us consider the linear case:

$$z_0(t) = e^{2\pi i \nu_0 t} . \quad (\text{C.1})$$

The FT [see Eq. (29)] of this signal is

$$\phi_0(\nu) = \frac{\sin \pi(\nu_0 - \nu)N}{\pi(\nu_0 - \nu)N} \quad (\text{C.2})$$

and it can be expanded around the maximum ν_0 :

$$\phi_0(\nu) = \phi_0(\nu_0) + \frac{(\nu - \nu_0)^2}{2} \phi_0''(\nu_0) + O(\nu - \nu_0)^3 \quad \phi_0''(\nu_0) = -\frac{\pi^2 N^2}{3} . \quad (\text{C.3})$$

In the linear case, the position of the maximum of the FT coincides with the frequency ν_0 . If we add a perturbation made up of a sinusoidal wave [see Eq. (A.1)], the FT reads

$$\phi(\nu) = \phi_0(\nu) + \phi_1(\nu) = \frac{\sin \pi(\nu_0 - \nu)N}{\pi(\nu_0 - \nu)N} + b_0 \frac{\sin \pi(\nu_1 - \nu)N}{\pi(\nu_1 - \nu)N} . \quad (\text{C.4})$$

We expand the derivative of the FT around ν_0 in order to evaluate the shift in the main peak due to the secondary frequency:

$$\frac{d\phi}{d\nu} = \phi_1'(\nu_0) + (\nu - \nu_0)(\phi_0''(\nu_0) + \phi_1''(\nu_0)) + O(\nu - \nu_0)^2 ; \quad (\text{C.5})$$

setting the derivative to zero, one obtains the FT estimate:

$$\nu_{FT} = \nu_0 - \frac{\phi_1'(\nu_0)}{\phi_0''(\nu_0) + \phi_1''(\nu_0)} = \nu_0 - \frac{\phi_1'(\nu_0)}{\frac{\pi^2 N^2}{3} - \phi_1''(\nu_0)} . \quad (\text{C.6})$$

We assume that $\Delta\nu = \nu_0 - \nu_1$ is $O(1)$, and we expand in powers of N^{-1} : since $\phi_1'(\nu_0)$ is $O(1)$ and $\phi_1''(\nu_0)$ is $O(N)$, one has

$$\nu_{FT} = \nu_0 - \frac{3\phi_1'(\nu_0)}{\pi^2} \frac{1}{N^2} + O(N^{-3}) \quad (\text{C.7})$$

and therefore the error estimate is

$$|\epsilon_{FT}| \leq \frac{C_{FT}}{N^2} \quad C_{FT} = \frac{3\phi_1'(\nu_0)}{\pi^2} . \quad (\text{C.8})$$

If $\Delta\nu$ is small compared to the inverse of the number of samples, one can prove that in the limit $\Delta\nu N \ll 1$ the error is independent of N , and one obtains the same estimate as for the APA method [see Eq. (A.9)]. The same kind of analysis can be carried out for a signal of type 2), with complex amplitudes.

C.2 FT with Hanning Filter

We consider a weight function χ , and we define the FT in the continuous case as

$$\phi(\nu) = \frac{1}{N} \int_{-N/2}^{N/2} e^{-2\pi i \nu t} z(t) \chi(t) dt ; \quad (\text{C.9})$$

we analyse the case of a Hanning filter [see Sect. 4.3.2], which for a signal defined in $t \in [-N/2, N/2]$ reads

$$\chi(t) = \cos\left(\frac{\pi t}{N}\right). \quad (\text{C.10})$$

The FT in the linear case is

$$\phi(\nu) = -\frac{1}{\pi N^3} \frac{\sin \pi(\nu_0 - \nu)N}{(\nu_0 - \nu) \left((\nu - \nu_0)^2 - \frac{1}{N^2} \right)}. \quad (\text{C.11})$$

One can carry out the same analysis as in Appendix B.2 for a weakly perturbed orbit [see Eq. (A.1)]: the first equality of Eq. (C.6) still holds, but in this case the derivatives of ϕ satisfy the following scaling laws

$$\phi_0''(\nu_0) = O(N^2) \quad \phi_1'(\nu_0) = O(N^{-2}) \quad \phi_1''(\nu_0) = O(N^{-1}) \quad (\text{C.12})$$

and therefore in the case $N \gg 1$, $N\Delta\nu \gg 1$ one has

$$|\epsilon_{FTH}| \leq \frac{C_{FTH}}{N^4}. \quad (\text{C.13})$$

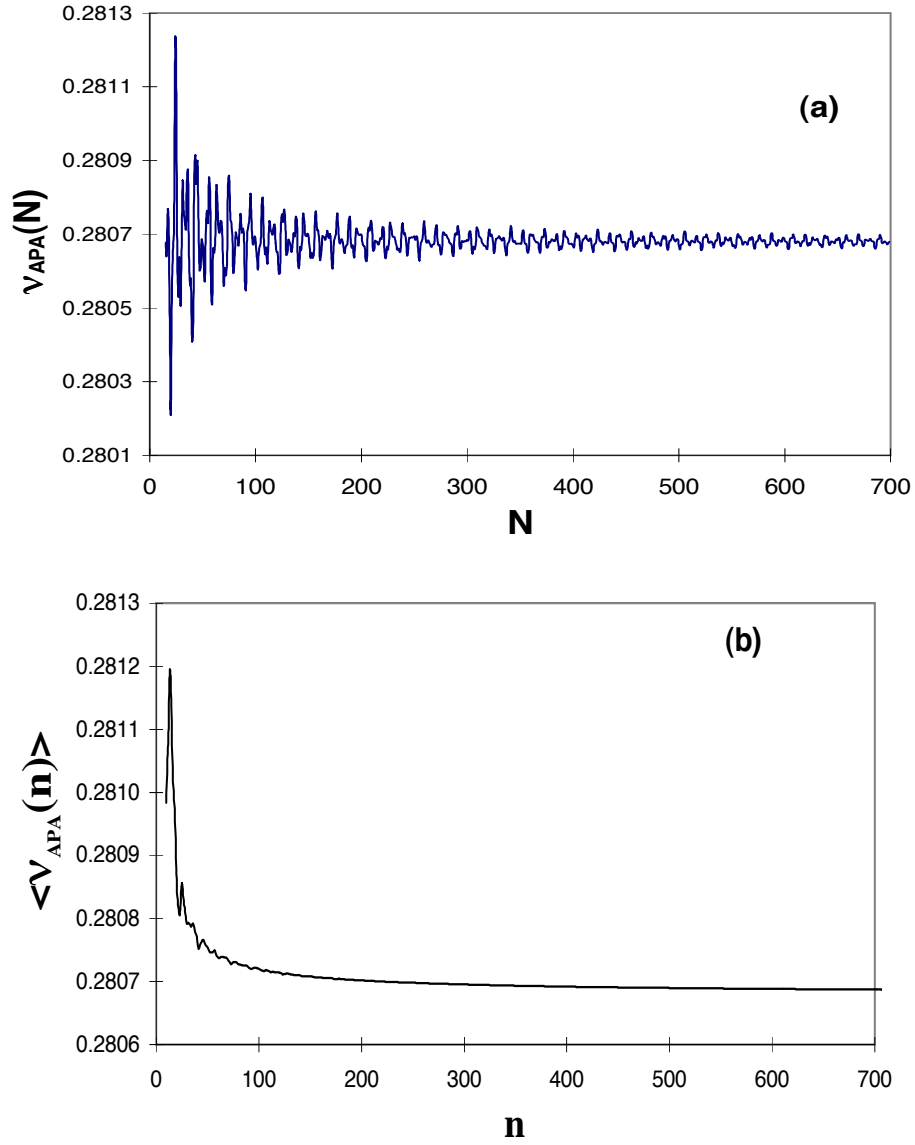


FIGURE 1: Tune computed as the Average Phase Advance as a function of the number of samples N for a sine wave [see Eq. (2)] with four harmonics (a). Averaged tune $\langle \nu_{APA}(n) \rangle$ versus n for the same signal (b).

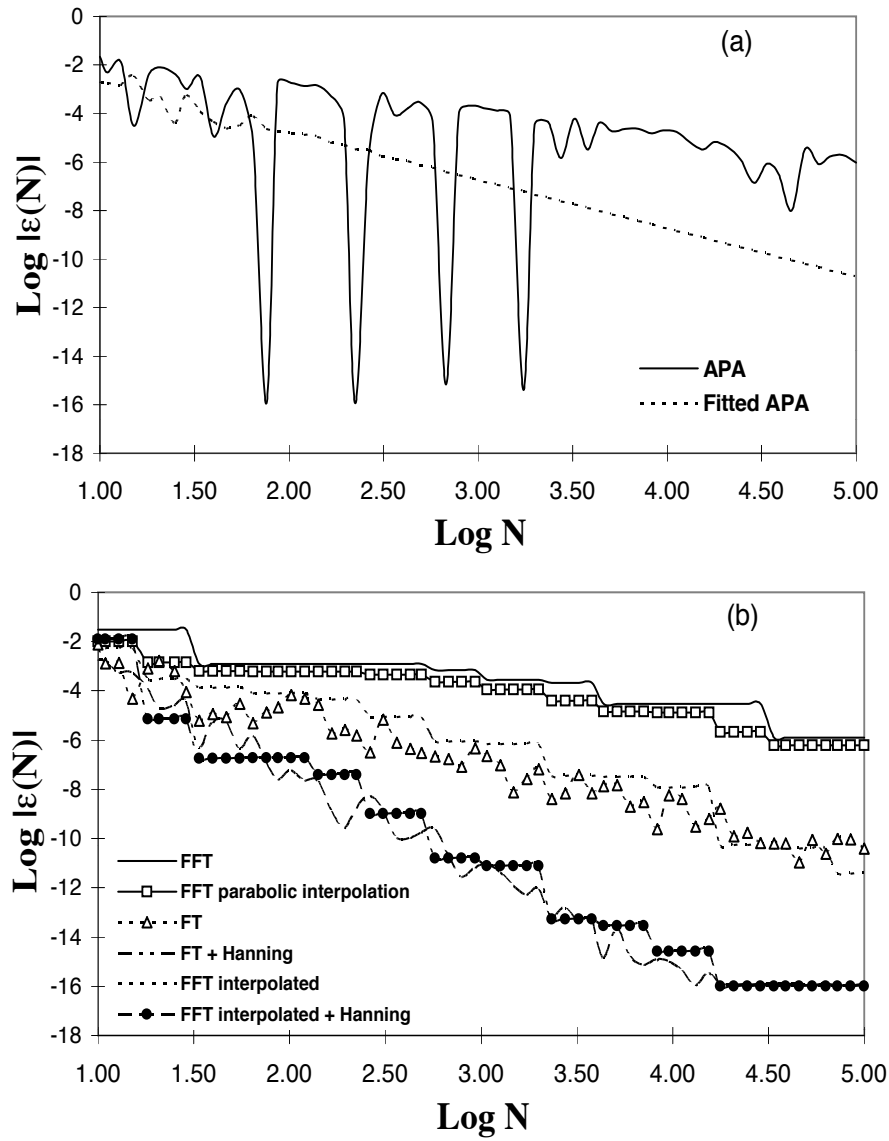


FIGURE 2: Tune error $\epsilon(N)$ versus N for the APA methods (a) and for the Fourier methods (b); the signal is generated by one sine wave with four harmonics [see Eq. (2)].

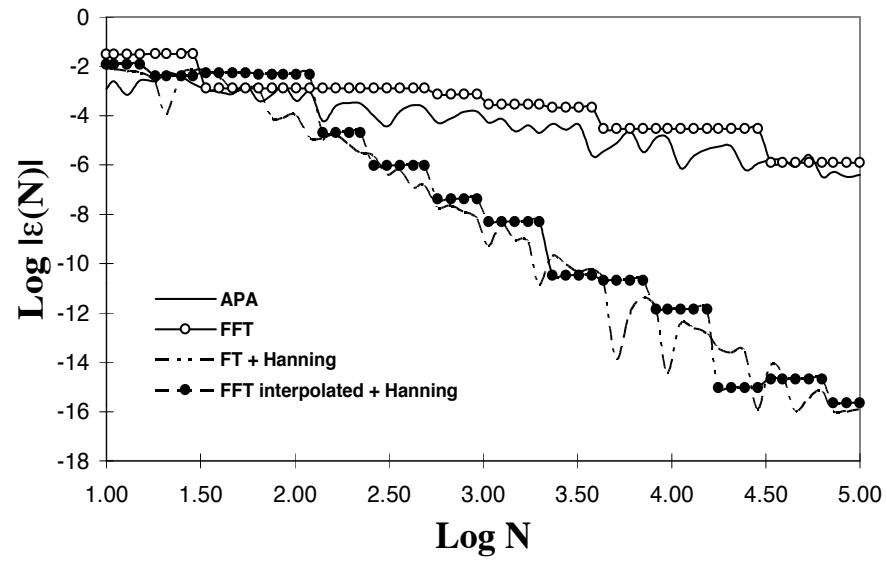


FIGURE 3: Tune error $\epsilon(N)$ versus N for different methods. The signal is generated by two sine waves with four harmonics each [see Eq. (3)], with $\nu_0 = 0.28$ and $\nu_1 = 0.31$.

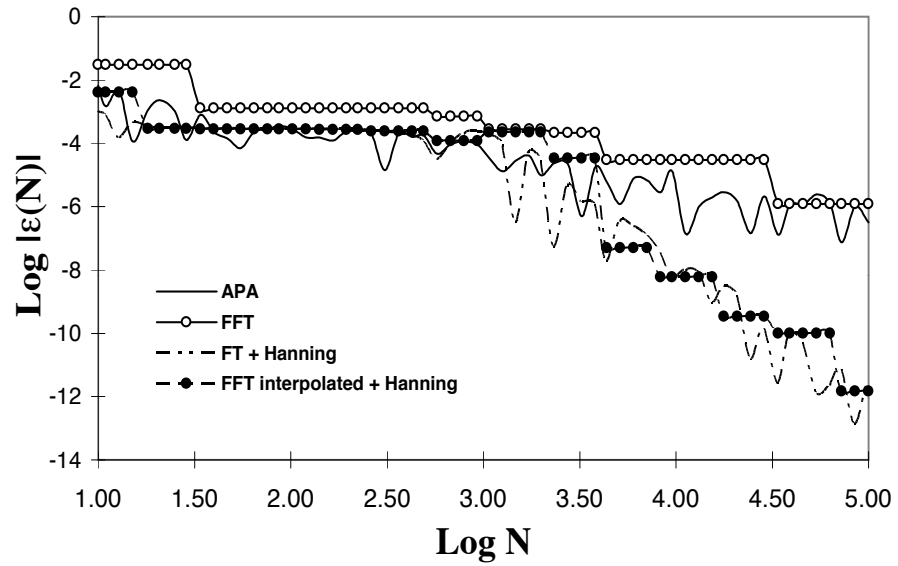


FIGURE 4: Tune error $\epsilon(N)$ versus N for different methods. The signal is generated by two sine waves with four harmonics each [see Eq. (3)], with $\nu_0 = 0.28$ and $\nu_1 = 0.281$.

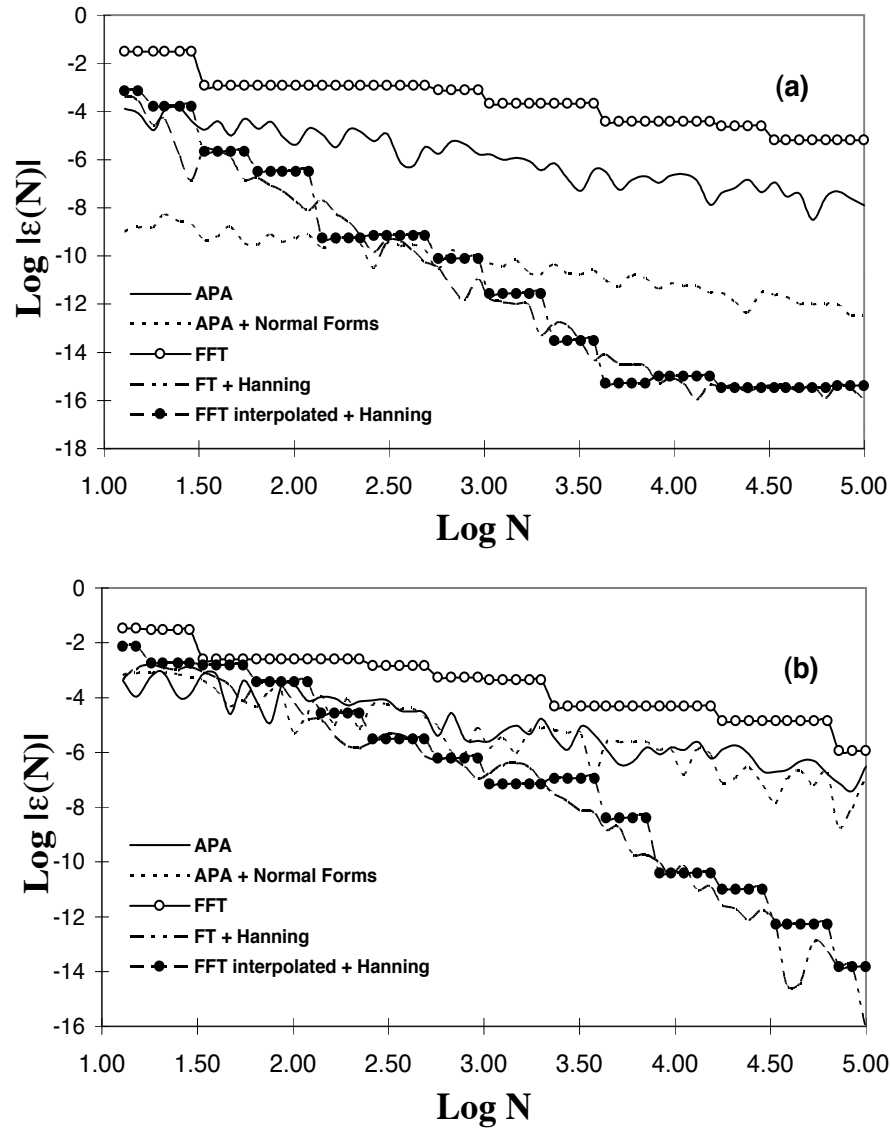


FIGURE 5: Tune error $\epsilon(N)$ as a function of N for an orbit of the 4D Hénon map with $\nu_x = 0.28$ and $\nu_y = 0.31$: initial condition close to the origin (a) and close to the dynamic aperture (b). A selection of the described methods is shown.

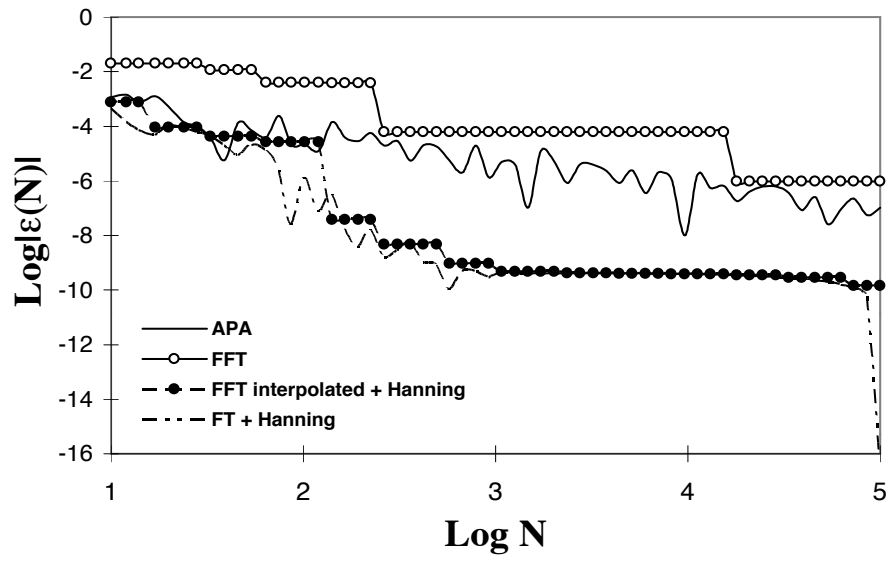


FIGURE 6: Tune error $\epsilon(N)$ versus N for a simulation of an orbit of the SPS lattice with initial condition at half of the dynamic aperture. A selection of the described methods is shown.

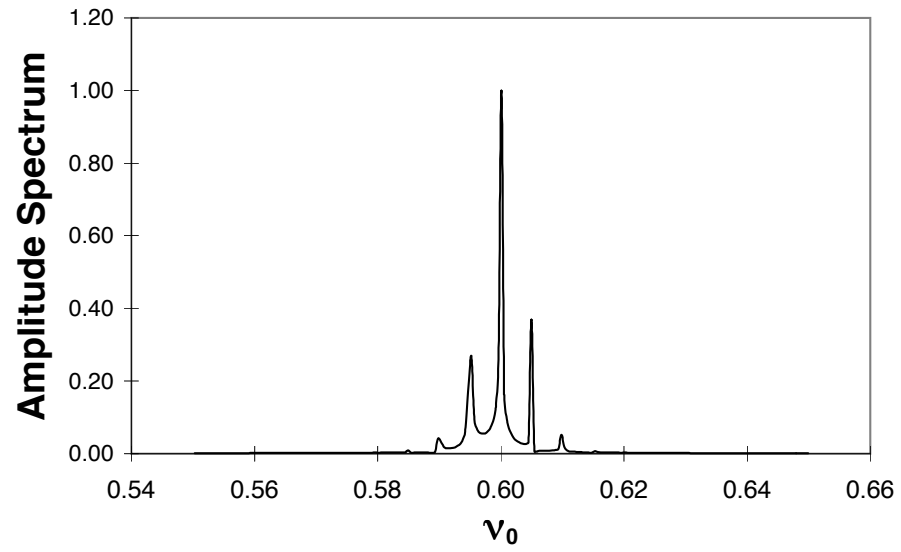


FIGURE 7: FFT of a signal of a modulated sine wave [see Eq. (4)].

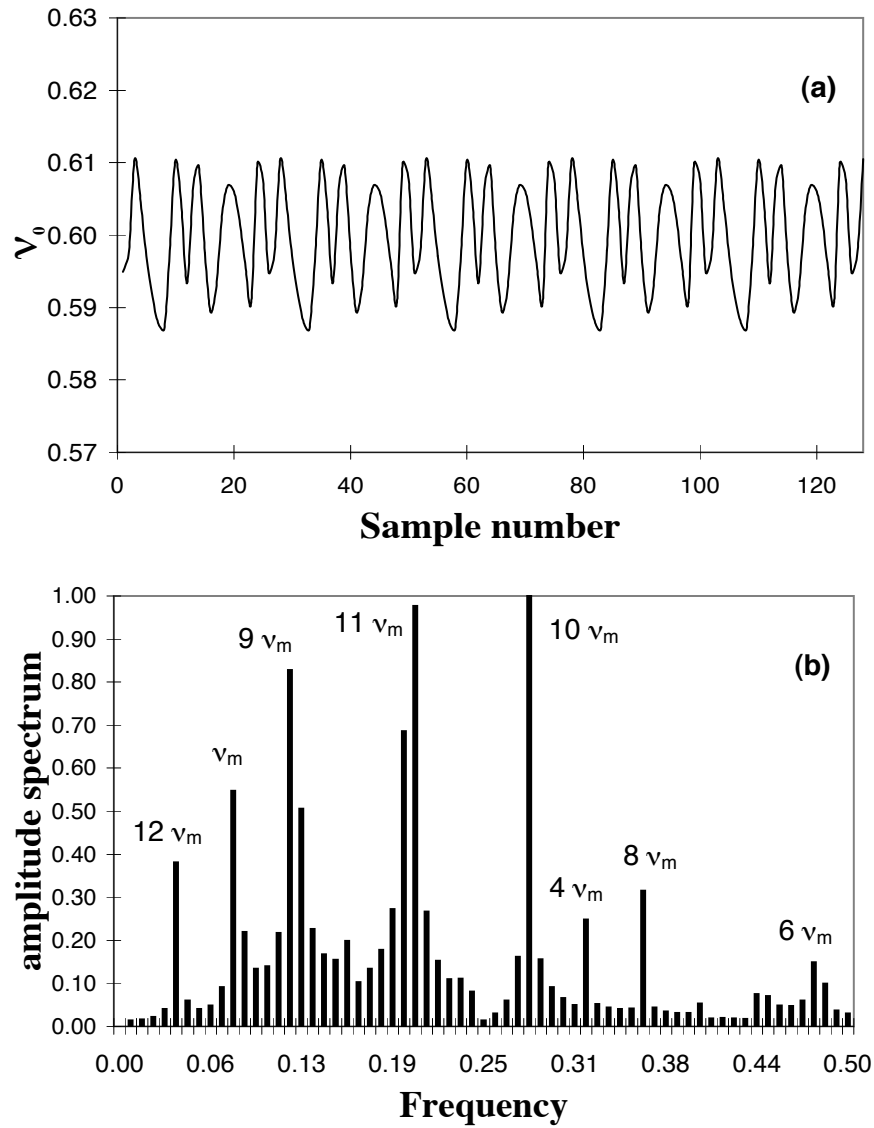


FIGURE 8: Tune value for a sine wave with modulated frequency [see Eq. (4)] computed over short samples of length $n = 16$ (a); FFT of the tune dependence on the number of samples (b).

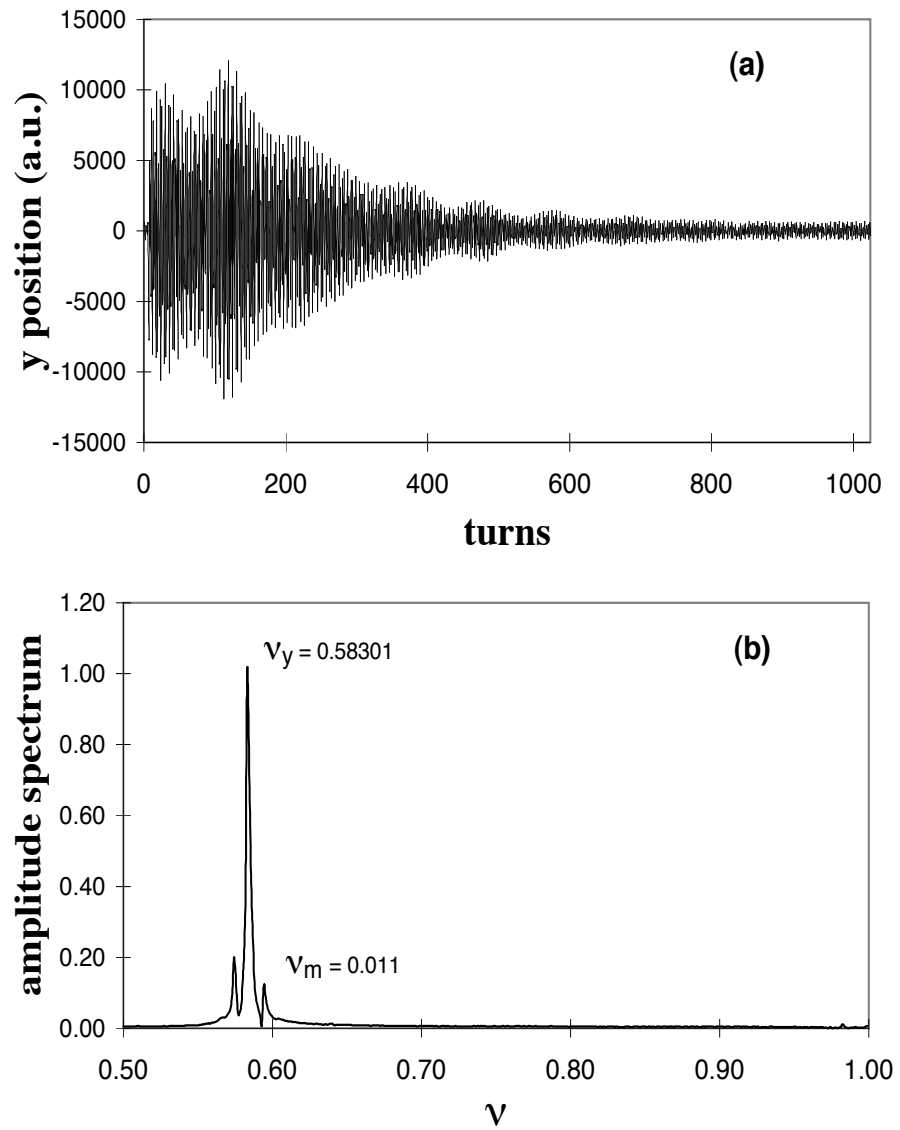


FIGURE 9: Position of the beam versus number of turns for a proton beam at SPS (a); FFT of the above signal (b).

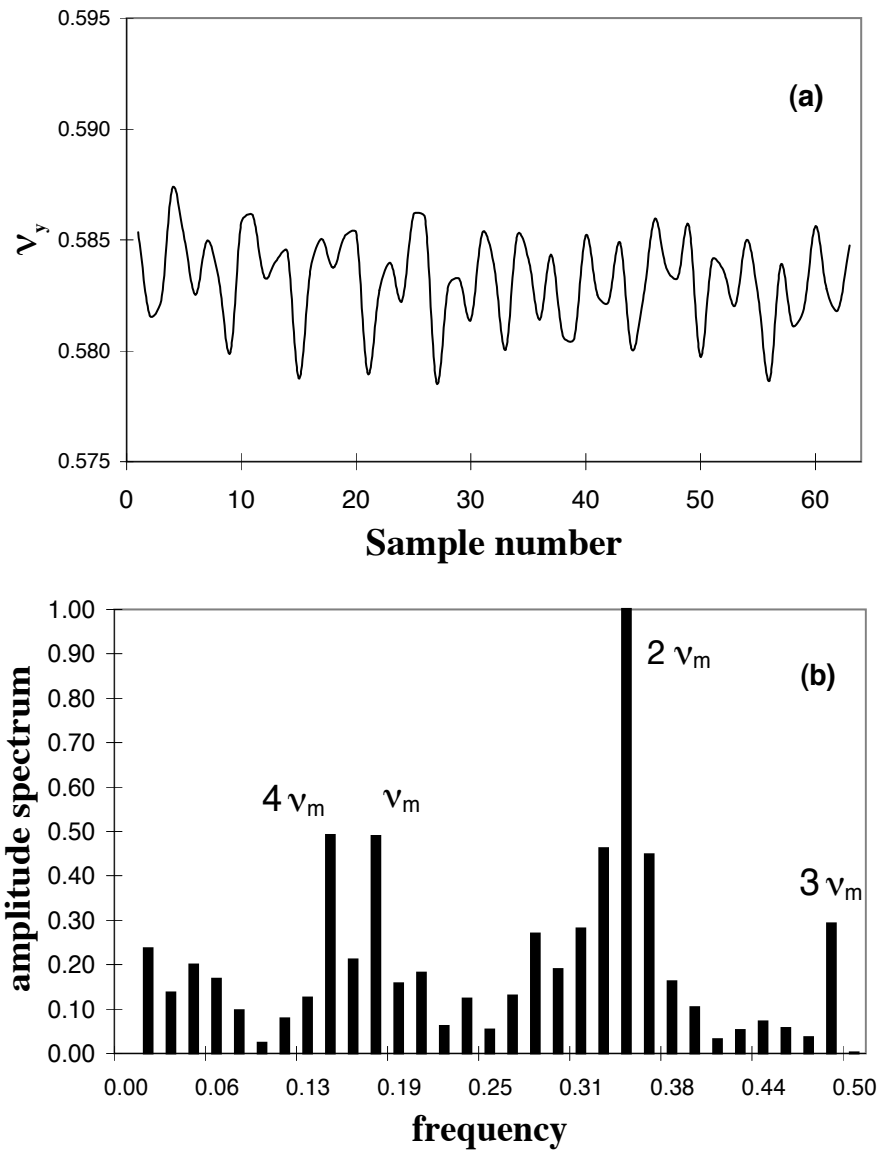


FIGURE 10: Tune value for the experimental signal of a SPS proton beam computed over short samples of length $n = 16$ (a); FFT of the tune dependence on the number of samples (b).